

AD-A079 613

AEROSPACE CORP EL SEGUNDO CA AEROPHYSICS LAB
02 (1 DELTA)-I ATOM KINETIC STUDIES.(U)

F/6 7/4

NOV 79 R F HEIDNER, C E GARDNER

F04701-79-C-0080

UNCLASSIFIED

TR-0080(5606)-2

SD-TR-79-6

NL

[OF]
[A]
[C] [D] [E] [F] [G] [H] [I] [J] [K] [L] [M] [N] [O] [P] [Q] [R] [S] [T] [U] [V] [W] [X] [Y] [Z] [AA] [AB] [AC] [AD] [AE] [AF] [AG] [AH] [AI] [AJ] [AK] [AL] [AM] [AN] [AO] [AP] [AQ] [AR] [AS] [AT] [AU] [AV] [AW] [AX] [AY] [AZ] [BA] [BB] [BC] [BD] [BE] [BF] [BG] [BH] [BI] [BJ] [BK] [BL] [BM] [BN] [BO] [BP] [BQ] [BR] [BS] [BT] [BU] [BV] [BW] [BX] [BY] [BZ] [CA] [CB] [CC] [CD] [CE] [CF] [CG] [CH] [CI] [CJ] [CK] [CL] [CM] [CN] [CO] [CP] [CQ] [CR] [CS] [CT] [CU] [CV] [CW] [CX] [CY] [CZ] [DA] [DB] [DC] [DD] [DE] [DF] [DG] [DH] [DI] [DJ] [DK] [DL] [DM] [DN] [DO] [DP] [DQ] [DR] [DS] [DT] [DU] [DV] [DW] [DX] [DY] [DZ] [EA] [EB] [EC] [ED] [EE] [EF] [EG] [EH] [EI] [EJ] [EK] [EL] [EM] [EN] [EO] [EP] [EQ] [ER] [ES] [ET] [EU] [EV] [EW] [EX] [EY] [EZ] [FA] [FB] [FC] [FD] [FE] [FF] [FG] [FH] [FI] [FJ] [FK] [FL] [FM] [FN] [FO] [FP] [FQ] [FR] [FS] [FT] [FU] [FV] [FW] [FX] [FY] [FZ] [GA] [GB] [GC] [GD] [GE] [GF] [GG] [GH] [GI] [GJ] [GK] [GL] [GM] [GN] [GO] [GP] [GQ] [GR] [GS] [GT] [GU] [GV] [GW] [GX] [GY] [GZ] [HA] [HB] [HC] [HD] [HE] [HF] [HG] [HH] [HI] [HJ] [HK] [HL] [HM] [HN] [HO] [HP] [HQ] [HR] [HS] [HT] [HU] [HV] [HW] [HX] [HY] [HZ] [IA] [IB] [IC] [ID] [IE] [IF] [IG] [IH] [II] [IJ] [IK] [IL] [IM] [IN] [IO] [IP] [IQ] [IR] [IS] [IT] [IU] [IV] [IW] [IX] [IY] [IZ] [JA] [JB] [JC] [JD] [JE] [JF] [JG] [JH] [JI] [JJ] [JK] [JL] [JM] [JN] [JO] [JP] [JQ] [JR] [JS] [JT] [JU] [JV] [JW] [JX] [JY] [JZ] [KA] [KB] [KC] [KD] [KE] [KF] [KG] [KH] [KI] [KJ] [KK] [KL] [KM] [KN] [KO] [KP] [KQ] [KR] [KS] [KT] [KU] [KV] [KW] [KX] [KY] [KZ] [LA] [LB] [LC] [LD] [LE] [LF] [LG] [LH] [LI] [LJ] [LK] [LL] [LM] [LN] [LO] [LP] [LQ] [LR] [LS] [LT] [LU] [LV] [LW] [LX] [LY] [LZ] [MA] [MB] [MC] [MD] [ME] [MF] [MG] [MH] [MI] [MJ] [MK] [ML] [MM] [MN] [MO] [MP] [MQ] [MR] [MS] [MT] [MU] [MV] [MW] [MX] [MY] [MZ] [NA] [NB] [NC] [ND] [NE] [NF] [NG] [NH] [NI] [NJ] [NK] [NL] [NM] [NN] [NO] [NP] [NQ] [NR] [NS] [NT] [NU] [NV] [NW] [NX] [NY] [NZ] [OA] [OB] [OC] [OD] [OE] [OF] [OG] [OH] [OI] [OJ] [OK] [OL] [OM] [ON] [OO] [OP] [OQ] [OR] [OS] [OT] [OU] [OV] [OW] [OX] [OY] [OZ] [PA] [PB] [PC] [PD] [PE] [PF] [PG] [PH] [PI] [PJ] [PK] [PL] [PM] [PN] [PO] [PP] [PQ] [PR] [PS] [PT] [PU] [PV] [PW] [PX] [PY] [PZ] [QA] [QB] [QC] [QD] [QE] [QF] [QG] [QH] [QI] [QJ] [QK] [QL] [QM] [QN] [QO] [QP] [QQ] [QR] [QS] [QT] [QU] [QV] [QW] [QX] [QY] [QZ] [RA] [RB] [RC] [RD] [RE] [RF] [RG] [RH] [RI] [RJ] [RK] [RL] [RM] [RN] [RO] [RP] [RQ] [RR] [RS] [RT] [RU] [RV] [RW] [RX] [RY] [RZ] [SA] [SB] [SC] [SD] [SE] [SF] [SG] [SH] [SI] [SJ] [SK] [SL] [SM] [SN] [SO] [SP] [SQ] [SR] [SS] [ST] [SU] [SV] [SW] [SX] [SY] [SZ] [TA] [TB] [TC] [TD] [TE] [TF] [TG] [TH] [TI] [TJ] [TK] [TL] [TM] [TN] [TO] [TP] [TQ] [TR] [TS] [TT] [TU] [TV] [TW] [TX] [TY] [TZ] [UA] [UB] [UC] [UD] [UE] [UF] [UG] [UH] [UI] [UJ] [UK] [UL] [UM] [UN] [UO] [UP] [UQ] [UR] [US] [UT] [UU] [UV] [UW] [UX] [UY] [UZ] [VA] [VB] [VC] [VD] [VE] [VF] [VG] [VH] [VI] [VJ] [VK] [VL] [VM] [VN] [VO] [VP] [VQ] [VR] [VS] [VT] [VU] [VV] [VW] [VX] [VY] [VZ] [WA] [WB] [WC] [WD] [WE] [WF] [WG] [WH] [WI] [WJ] [WK] [WL] [WM] [WN] [WO] [WP] [WQ] [WR] [WS] [WT] [WU] [WV] [WW] [WX] [WY] [WZ] [XA] [XB] [XC] [XD] [XE] [XF] [XG] [XH] [XI] [XJ] [XK] [XL] [XM] [XN] [XO] [XP] [XQ] [XR] [XS] [XT] [XU] [XV] [XW] [XX] [XY] [XZ] [YA] [YB] [YC] [YD] [YE] [YF] [YG] [YH] [YI] [YJ] [YK] [YL] [YM] [YN] [YO] [YP] [YQ] [YR] [YS] [YT] [YU] [YV] [YW] [YX] [YY] [YZ] [ZA] [ZB] [ZC] [ZD] [ZE] [ZF] [ZG] [ZH] [ZI] [ZJ] [ZK] [ZL] [ZM] [ZN] [ZO] [ZP] [ZQ] [ZR] [ZS] [ZT] [ZU] [ZV] [ZW] [ZX] [ZY] [ZZ]

2 - 80

END

DATE

FILED

2 - 80

DDC

AD A 079613

12
5

LEVEL

$O_2(^1\Delta)$ -I Atom Kinetic Studies

R. F. HEIDNER and C. E. GARDNER
Aerophysics Laboratory
Laboratory Operations
El Segundo, Calif. 90245

8 November 1979

Interim Report

DDC
RECEIVED
JAN 18 1980
A

APPROVED FOR PUBLIC RELEASE;
DISTRIBUTION UNLIMITED

Prepared for

AIR FORCE WEAPONS LABORATORY
Kirtland Air Force Base, N. Mex. 87117

SPACE DIVISION
AIR FORCE SYSTEMS COMMAND
Los Angeles Air Force Station
P.O. Box 92960, Worldway Postal Center
Los Angeles, Calif. 90009


FILE COPY

1 17 009

This interim report was submitted by The Aerospace Corporation, El Segundo, CA 90245, under Contract No. F04701-79-C-0080 with the Space Division, Deputy for Technology, P.O. Box 92960, Worldway Postal Center, Los Angeles, CA 90009. It was reviewed and approved for The Aerospace Corporation by W. R. Warren, Jr., Aerophysics Laboratory. Lieutenant J. C. Garcia, SAMSO/DYXT, was the project officer for Technology.

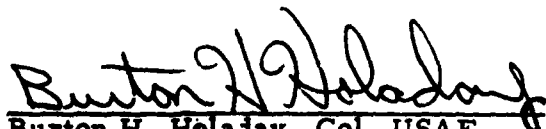
This report has been reviewed by the Information Office (OI) and is releasable to the National Technical Information Service (NTIS). At NTIS, it will be available to the general public, including foreign nations.

This technical report has been reviewed and is approved for publication. Publication of this report does not constitute Air Force approval of the report's findings or conclusions. It is published only for the exchange and stimulation of ideas.


James C. Garcia, Lt, USAF
Project Officer


Joseph J. Cox, Lt Col, USAF
Chief, Advanced Technology Division

FOR THE COMMANDER


Burton H. Holaday, Col, USAF
Director of Technology Plans
and Analysis
Deputy for Technology

UNCLASSIFIED

SECURITY CLASSIFICATION OF THIS PAGE (When Data Entered)

19 REPORT DOCUMENTATION PAGE		READ INSTRUCTIONS BEFORE COMPLETING FORM
1. REPORT NUMBER (18) SD-TR-79-6 (1 Delta)	2. GOVT ACCESSION NO.	3. RECIPIENT'S CATALOG NUMBER
4. TITLE (and Subtitle) (6) O ₂ (¹ Δ)-I ATOM KINETIC STUDIES.	5. TYPE OF REPORT & PERIOD COVERED (9) Interim rept.	
7. AUTHOR(s) (10) Raymond F. Heidner III and Carrol E. Gardner	6. PERFORMING ORG. REPORT NUMBER (14) TR-0080(5606)-2	
9. PERFORMING ORGANIZATION NAME AND ADDRESS The Aerospace Corporation El Segundo, Calif. 90245	8. CONTRACT OR GRANT NUMBER(s) (15) F04701-79-C-0080 ^{Ken}	
11. CONTROLLING OFFICE NAME AND ADDRESS Air Force Weapons Laboratory Kirtland Air Force Base, New Mex. 87117	10. PROGRAM ELEMENT, PROJECT, TASK AREA & WORK UNIT NUMBERS (12) 41	
14. MONITORING AGENCY NAME & ADDRESS (if different from Controlling Office) Space Division Air Force Systems Command Los Angeles, Calif. 90009	12. REPORT DATE (11) 8 Nov 1979	
15. SECURITY CLASS. (of this report) Unclassified	13. NUMBER OF PAGES 39	
16. DISTRIBUTION STATEMENT (of this Report) Approved for public release; distribution unlimited	15a. DECLASSIFICATION/DOWNGRADING SCHEDULE	
17. DISTRIBUTION STATEMENT (of the abstract entered in Block 20, if different from Report)		
18. SUPPLEMENTARY NOTES		
19. KEY WORDS (Continue on reverse side if necessary and identify by block number) Electronically Excited Oxygen Electronic Energy Transfer Flow-Tube Kinetic Studies Gas Mixing CW Iodine Laser 1Δ = 1 sub DELTA 1Σ = 1 sub sigma (O ₂ (¹ Δ) I sub DELTA) 20 TH 2ND POWER		
20. ABSTRACT (Continue on reverse side if necessary and identify by block number) A discharge flow system has been used to refine kinetic rate measurements for the O ₂ (¹ Δ) + I [*] energy-pooling process and for the iodine-catalyzed removal of O ₂ (¹ Δ). Particular attention was given the effects of I ₂ -carrier gas (Ar) on the emission intensity of O ₂ (¹ Δ) and O ₂ (¹ Σ). A heated I ₂ saturator and a saturator bypass technique were developed to minimize such effects. The data reported here indicate that processes proportional to [O ₂ (¹ Δ)] ² are important at [O ₂ (¹ Δ)] and [I [*]] densities, which are appropriate for a cw O ₂ (¹ Δ)-I atom transfer laser.		

CONTENTS

I.	INTRODUCTION	7
II.	EXPERIMENTAL	11
III.	RESULTS	17
	A. Influence of Injected Ar on $O_2(^1\Delta, ^1\Sigma)$ Intensity Measurements	17
	B. Energy Pooling of I^* with $O_2(^1\Delta)$	20
	C. Iodine Catalyzed Removal of $O_2(^1\Delta)$	26
IV.	DISCUSSION	35
V	CONCLUSIONS	39
APPENDIXES		
	A. Chemical Kinetics of the $O_2(^1\Delta)$ -I Atom System	41
	B. Rate Coefficients for the Kinetic Model of Appendix A	43

Accession For	
NTIS GR&I	<input checked="" type="checkbox"/>
DLC TAB	<input type="checkbox"/>
Unprocessed	<input type="checkbox"/>
Justified	<input type="checkbox"/>
Dist	Available for special
A	

FIGURES

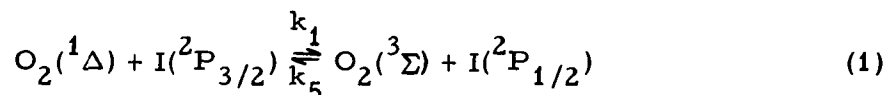
1.	Electronic Energy Levels in O_2-I_2 System	8
2.	I_2 Dissociation Cycle in $O_2(^1\Delta)$ -I Atom Transfer System . . .	9
3.	Schematic of $O_2^*-I^*$ Diagnostic Methods	12
4.	Vapor-Pressure Curve for I_2	14
5.	Variation of $O_2(^1\Delta, ^1\Sigma)$ Emission with Ar Injection	18
6.	Effect of Ar on I_{6340} Versus $[O_2(^1\Delta)]^2$	19
7.	Determination of k_2 without Saturator Bypass Technique	23
8.	Determination of k_2 by Use of Saturator Bypass Technique . .	25
9.	Time-Dependent $O_2(^1\Delta)$ Dimol and $O_2(^1\Sigma)$ Emission in the Presence of I_2	28
10.	Time-Dependent First-Order Decay of $O_2(^1\Delta)$ ($\lambda = 1.27 \mu m$) Versus I_2	29
11.	Determination of k_{eff} with First-Order Decay of $O_2(^1\Delta)$ Assumed	31
12.	Time-Dependent Second-Order Decay of $O_2(^1\Delta)$ ($\lambda = 1.27 \mu m$) Versus I_2	32
13.	Determination of $k_2 + k'_2$ with Second-Order Decay Kinetics Assumed for $O_2(^1\Delta)$	33

TABLES

I.	Spectroscopy of the O_2 -I Atom Transfer System	13
II.	Flow System Reactant Contact Time	16
III.	Comparison of Kinetic Results	34

I. INTRODUCTION

Workers at AFWL recently demonstrated an efficient, chemically pumped, cw electronic transition laser that is based on the $O_2(^1\Delta)$ -I atom transfer system.¹



The intent in this technical report is to supplement and, where necessary, to revise the conclusions reached in earlier studies on this transfer system.² The nomenclature and rate-coefficient numbering scheme introduced in the pioneering studies by Derwent and Thrush³⁻⁷ are used in this report. For reference, the relevant spectroscopic energy levels and the logic flow chart of the $O_2(^1\Delta)$ -I atom transfer system are reproduced from Reference 2 and appear as Figs. 1 and 2.

¹W. E. McDermott, N. R. Pchelkin, D. J. Benard, and R. R. Bousek, "An Electronic Transition Chemical Laser," Appl. Phys. Lett. **32**, 469 (1978).

²R. F. Heidner III, J. G. Coffey, and C. E. Gardner, $O_2(^1\Delta)$ - I Atom Energy-Transfer Studies: CW Inversion on 1.315 μ m I-Atom Transition, TR-0078(3610)-1, The Aerospace Corporation, El Segundo, Calif. (15 Dec. 1977).

³R. G. Derwent, D. R. Kearns, and B. A. Thrush, "The Excitation of Iodine by Singlet Molecular Oxygen," Chem. Phys. Lett. **6**, 115 (1970).

⁴R. G. Derwent and B. A. Thrush, "Measurements on $O_2(^1\Delta_g)$ and $O_2(^1\Sigma^+)$ in Discharge Flow Systems," Trans. Faraday Soc. **67**, 2036 (1971).

⁵R. G. Derwent and B. A. Thrush, "The Radiative Lifetime of the Metastable Iodine Atom $I(5^2P_{1/2})$," Chem. Phys. Lett. **9**, 591 (1971).

⁶R. G. Derwent and B. A. Thrush, "Excitation of Iodine by Singlet Molecular Oxygen," J. Chem. Faraday Soc. **II 68**, 720 (1972).

⁷R. G. Derwent and B. A. Thrush, "Excitation of Iodine by Singlet Molecular Oxygen," Disc. Faraday Soc. **53**, 162 (1972).

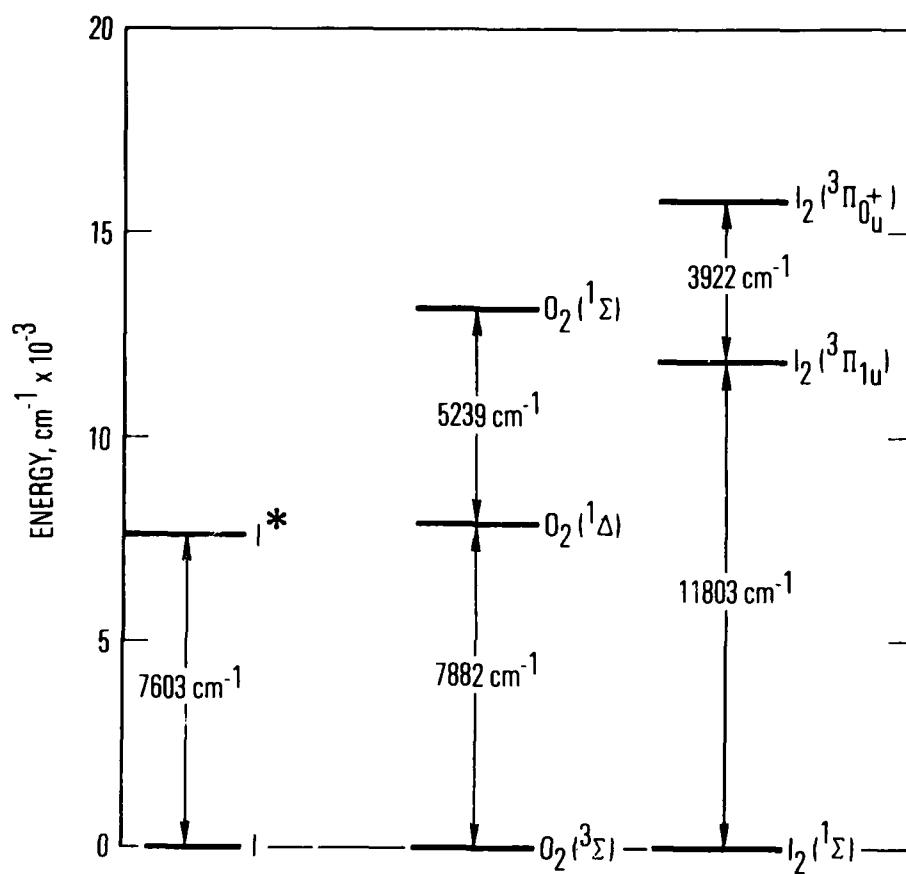


Fig. 1. Electronic Energy Levels in O₂-I₂ System

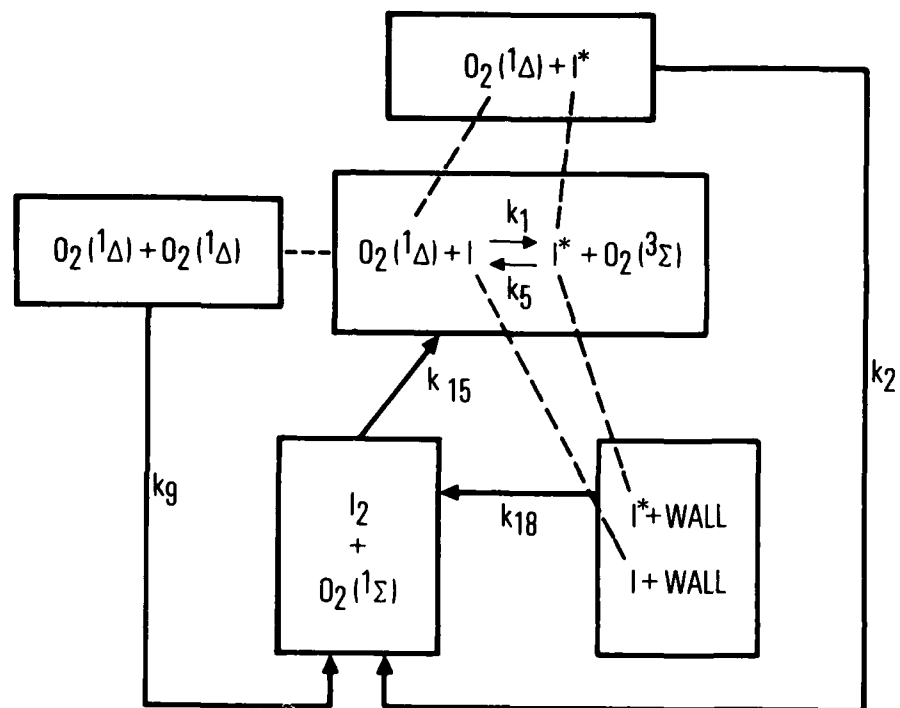


Fig. 2. I_2 Dissociation Cycle in $O_2(^1\Delta)$ -I Atom Transfer System

In this study, refined experimental methods were used, and conclusions quite different from those of Derwent and Thrush were reached. These new observations are of critical importance in the continued development of the cw I^* laser that is based on energy transfer from $O_2(^1\Delta)$.

II. EXPERIMENTAL

The experimental apparatus is depicted in Fig. 3. $O_2(^1\Delta)$ is produced by a microwave discharge in pure O_2 , and the O atoms that are simultaneously produced recombine on a heated HgO surface. The absolute concentration of $O_2(^1\Delta)$ was measured by means of an isothermal calorimeter method that is described in detail in Reference 2. Spectroscopic methods were calibrated against the probe measurements. The relevant spectroscopic features of the O_2 -I atom system are summarized in Table I.

The I_2 carrier gas was Ar. It flowed at atmospheric pressure through an I_2 saturator enclosed in an oven. A three-station digital thermocouple was used to monitor the temperature of the saturator. The Ar + I_2 was metered by means of a stainless steel needle valve held at a temperature several degrees warmer than the saturator. Partial pressures of I_2 in Ar were calculated from the vapor pressure data of Gillespie and Fraser (Fig. 4).⁸ Mole fractions of I_2 in Ar of $(5 - 10) \times 10^{-3}$ were obtained at saturator temperatures of 60 to 70°C.

The quality of the kinetic data was improved markedly when a "saturator-bypass" arrangement was used to inject the Ar + I_2 into the O_2 flow. This arrangement permitted a constant flow of Ar to be continuously injected into the O_2 stream and a measured fraction to be saturated with I_2 . Thus, the partial pressure of Ar in the flow remained constant while the concentration of injected I_2 was varied.

Two methods of obtaining decay plots of $O_2(^1\Delta)$, $O_2(^1\Sigma)$, and I^* were used. The Ar + I_2 could be shunted to one of three fixed injectors (A, B, or C), with the optical detectors used to monitor a fixed position on the flow tube. Alternatively, a single injector was used, and the detectors were

⁸L. J. Gillespie and L. H. D. Fraser, "The Normal Vapor Pressure of Crystalline Iodine," J. Am. Chem. Soc. **58**, 2260 (1936).

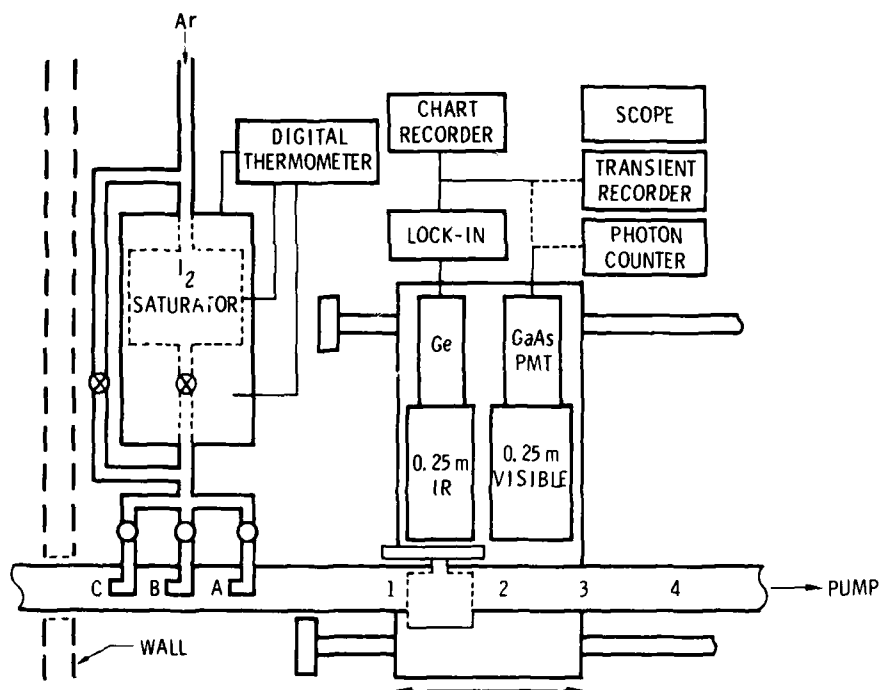


Fig. 3. Schematic of $O_2^*-I^*$ Diagnostic Methods

Table I. Spectroscopy of the O₂-I Atom Transfer System

Chemical Species	Electronic Transition	Observation Technique	Radiative Lifetime	Wavelength	Detector
O ₂ (¹ Δ)	a ¹ Δ _g → X ³ Σ _g ⁻	Emission	3660 sec ^a	1.27 μm	Ge (T = 77 K)
[O ₂ (¹ Δ) - O ₂ (¹ Δ)]	(a ¹ Δ, a ¹ Δ) → (X ³ Σ, X ³ Σ)	Emission	16 ± 4 cm ³ /mol-sec ^b	6340 Å	GaAs (T = 253 K) RCA 31034
O ₂ (¹ Σ)	b ¹ Σ _g ⁺ → X ³ Σ _g ⁻	Emission	13 sec ^c	7619 Å	GaAs (T = 253 K)
I ₂	B ³ Π _u ⁺ → X ¹ Σ _g ⁺	Emission	~5 × 10 ⁻⁷ sec ^d	5800 Å	GaAs (T = 253 K)
I*	2P _{1/2} → 2P _{3/2}	Emission	0.128 sec ^e	1.315 μm	Ge (T = 77 K)
I*	2P _{3/2} → 2P _{1/2}	Resonance Fluorescence	<3.6 nsec ^f	2062 Å	S-11 (T = 295 K) EMI 6256
I	4P _{5/2} → 2P _{3/2}	Resonance Fluorescence	90 ± 30 nsec ^f	1830 Å	S-11 (T = 295 K) EMI 6256

- R. M. Badger, A. C. Wright, and R. F. Whitlock, "Absolute Intensities of the Discrete and Continuous Absorption Bands of Oxygen Gas at 1.26 and 1.065 μ and the Radiative Lifetime of the 1Δ_g State of Oxygen," J. Chem. Phys. 43, 4345 (1965).
- R. G. Derwent and B. A. Thrush, "Measurements on O₂(¹Δ_g) and O₂(¹Σ_g⁺) in Discharge Flow Systems," Trans. Faraday Soc. 67, 2036 (1971).
- J. H. Miller, R. W. Boese, and L. P. Giver, "Intensity Measurements and Rotational Distributions for the Oxygen A-Band," J. Quantitative Spectroscopy Radiative Transfer 2, 1507 (1969).
- G. A. Capelle and H. P. Broida, "Lifetimes and Quenching Cross Sections of I₂(B³Π_u⁺)," J. Chem. Phys. 58, 4212 (1973).
- R. H. Garstang, "Transition Probabilities of Forbidden Lines," J. Res. NBS 68, 61 (1964).
- G. M. Lawrence, "Resonance Transition Probabilities in Intermediate Coupling for Some Neutral Non-Metals," Astrophys. J. 148, 261 (1967).

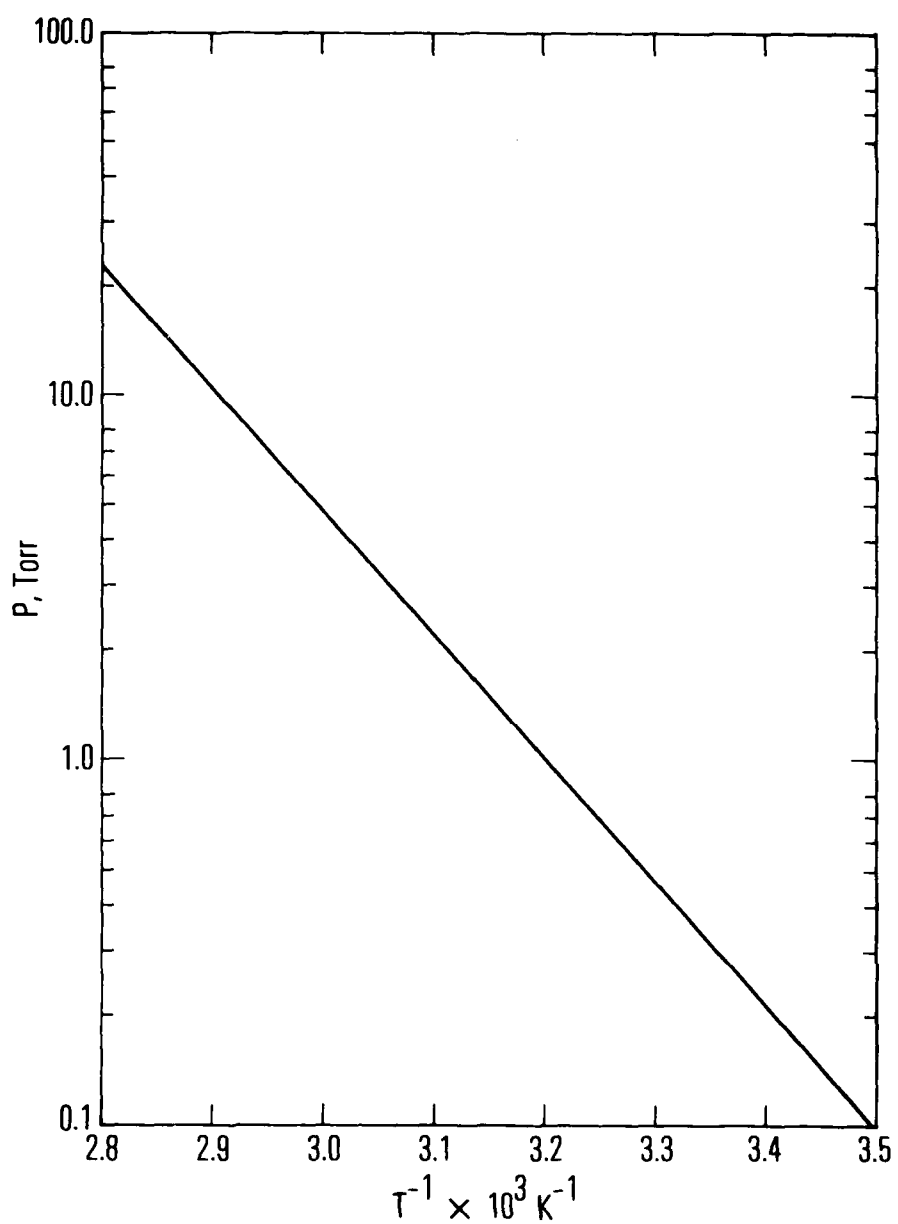


Fig. 4. Vapor-Pressure Curve for I₂ (Ref. 8)

translated along the flow tube (Positions 1, 2, 3, and 4) on a movable platform mounted on a ball bushing rail system (Thompson Co.). The relationship of the injector-detector positions to the contact time of the reactants is given in Table II, e.g., B-2 indicates that Injector B was used with the detector at Position 2.

The flow tube was made of square quartz (2.0 X 2.0 cm i.d.) and was internally coated with Halocarbon wax. Deposits of iodine oxides could be observed occasionally; however, mild external heating from a heat gun restored the original properties of the Halocarbon surface.

Table II. Flow System Reactant Contact Time^a

Detector Position ^b	Contact Time, msec		
	Injector Position		
	A	B	C
1	52	90	128
2	73	111	149
3	94	132	170
4	115	153	191

^aTable entries must be divided by the volume flow rate \dot{V} (l/sec) to obtain the contact time in milliseconds. Typically, $\dot{V} = 1.0$ l/sec.

^bSee Fig. 3.

III. RESULTS

A. INFLUENCE OF INJECTED Ar ON O₂(¹Δ, ¹Σ) INTENSITY MEASUREMENTS

In earlier experiments carried out in this Laboratory,² He was used as a carrier gas for I₂ instead of Ar. However, severe gas dynamic effects are possible when He is injected into O₂, because the viscosities are so different. It was hypothesized that the use of an Ar carrier would greatly alleviate this problem with only a small change in the partial pressure of O₂.

This hypothesis was explicitly tested by injecting Ar counter to the O₂ flow through L-shaped injectors (Fig. 3). Clyne⁹ evaluated the mixing times characteristic of similar arrangements. From his studies, a mixing time of 5 msec was predicted. The partial pressures of O₂ and Ar were calculated on the basis of complete mixing with the conventional formula

$$P_i = \left(\frac{\dot{m}_i}{\sum_i \dot{m}_i} \right) P_{TOT} \quad (2)$$

where the \dot{m}_i are molar flow rates.

The decay times of O₂(¹Δ) were essentially unchanged by the injection of Ar into the flow of active O₂. The intensity of both the "dimol" emission and the O₂(¹Σ) emission, both proportional to [O₂(¹Δ)]², decreased markedly with Ar addition; however, the ratio of these two intensities remained roughly constant (Fig. 5). Theoretically, a plot of I₆₃₄₀ versus [O₂(¹Δ)]² calculated from Eq. (2) should be a straight line; but, as demonstrated in Fig. 6, there is

⁹M. A. A. Clyne and H. W. Cruse, "Rates of Elementary Reactions Involving the BrO(X²π) and IO(X²π) Radicals," Trans. Faraday Soc. **66**, 2214 (1970).

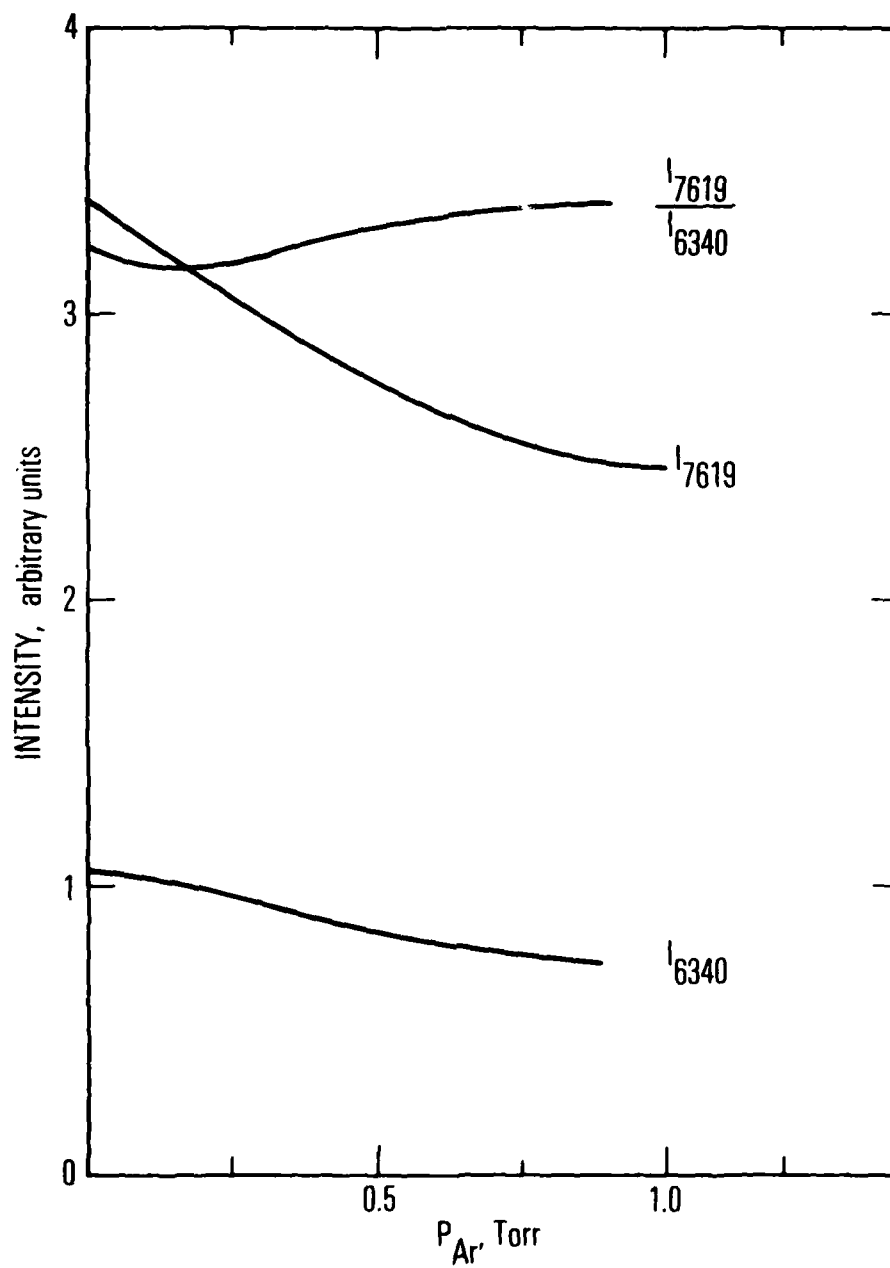


Fig. 5. Variation of O₂(¹Δ, ¹Σ) Emission with Ar Injection

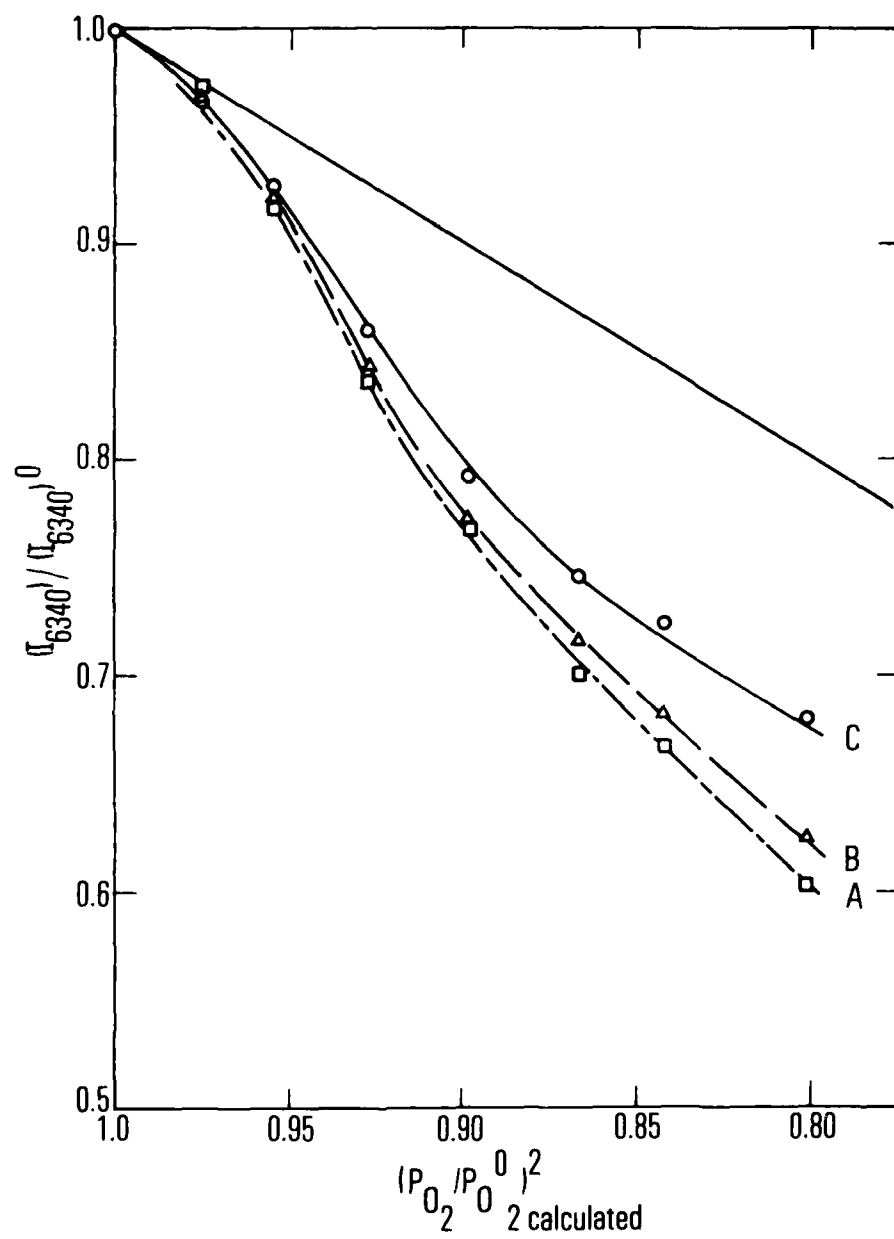


Fig. 6. Effect of Ar on I_{6340} Versus $[O_2(^1\Delta)]^2$

a substantial deviation from linearity. Three possible explanations for this behavior are:

1. The O_2 and Ar are not completely mixed.
2. The increase in system pressure with Ar addition has an effect on the $O_2(^1\Delta)$ production mechanism.
3. The addition of Ar has an effect on the dimol emission mechanism.

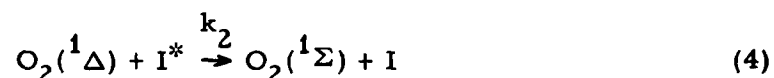
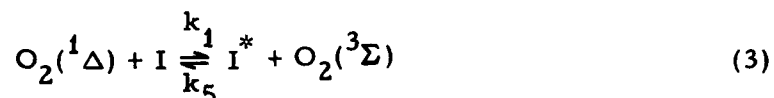
The first explanation is supported by the fact that the dimol emission increases as a constant mass flow of Ar is injected farther upstream ($A \rightarrow B \rightarrow C$). The measured intensity deviation from the gas dynamic predictions (25% low for $\dot{m}_{Ar}/\dot{m}_{O_2} = 0.4$) is rather small. The second explanation given may be valid also since the system pressure increases by approximately 25% for $\dot{m}_{Ar}/\dot{m}_{O_2} = 0.4$. Evidence for the third possibility has been cited recently at AFWL;* however, as demonstrated in Fig. 5, this effect is minor in the present system unless compensating errors exist for $O_2(^1\Sigma)$ and dimol emission.

The correct evaluation of the kinetic effect of I_2 (and therefore I atoms) on electronically excited O_2 requires that the amount of Ar carrier be limited to approximately 10 to 20% of the O_2 mass flow. This constraint mandates the saturation of the buffer gas stream with I_2 at elevated temperatures. The "saturator bypass" technique is equally important since it permits the mixing of Ar with O_2 to be identical as the partial pressure of I_2 in the Ar is increased. The total pressure is, thus, held constant, and, therefore, the discharge production of $O_2(^1\Delta)$ should also be constant.

B. ENERGY POOLING OF I^* WITH $O_2(^1\Delta)$

It is a generally accepted fact that $O_2(^1\Sigma)$ is enhanced by the addition of I_2 to a stream of electronically excited O_2 . The mechanism is as follows:

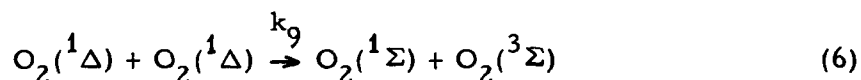
*D. Benard, private communication, 1978.



Unfortunately, earlier work in this Laboratory² and also by Derwent and Thrush³⁻⁷ failed to give the general analytic expression for the function $\text{O}_2(^1\Sigma) = f(\text{I}_2)$, which correctly describes the time-dependent removal of $\text{O}_2(^1\Delta)$ by I atoms. The simplest analytic approximation was derived in an earlier study, Eq. (B-13) of Reference 2, where $^1\Sigma^0$ represents the steady-state

$$\frac{^1\Sigma}{^1\Sigma^0} - 1 = \frac{k_2 k_1}{k_9(k_5 + k_6)} \frac{[\text{I}]}{[\text{O}_2(^3\Sigma)]} \quad (5)$$

concentration, which results from $\text{O}_2(^1\Delta)$ energy pooling with no I_2 , i. e.,



Two processes reduce the $[\text{O}_2(^1\Delta)]$ between the Ar + I_2 injector and the fluorescence region, thus reducing $\text{O}_2(^1\Sigma)^0$. They are:

1. The previously discussed gas dynamic perturbations caused by the Ar carrier gas introduced with the I_2 .
2. The I-atom catalyzed removal of $\text{O}_2(^1\Delta)$, which is discussed in the Section III. C.

Thus, a variation of Eq. (B-11) of Reference 2 must be applied in order to properly evaluate k_2 . Either of the following two expressions will provide proper analytical forms for determining k_2 :

$$\frac{I_{\Sigma}^0}{I_{\Sigma}^0} \left(\frac{I_{6340}^0}{I_{6340}} \right) - 1 = \frac{k_2 k_1}{k_9(k_5 + k_6)} \frac{[I]}{[O_2(^3\Sigma)]} \quad (7)$$

$$\frac{I_{\Sigma}^0}{I_{\Sigma}^0} \left(\frac{I_{1.27}^0}{I_{1.27}} \right)^2 - 1 = \frac{k_2 k_1}{k_9(k_5 + k_6)} \frac{[I]}{[O_2(^3\Sigma)]} \quad (8)$$

Two experimental approaches were applied to measuring k_2 . In the first approach, considerable data reduction and system modeling are required. It is presented in order to demonstrate the errors introduced by gas dynamic problems.

From Eq. (B-6) of Reference 2, the expression can be written

$$\frac{O_2(^1\Delta)^0}{O_2(^1\Delta)} = \left(\frac{I_{6340}^0}{I_{6340}} \right)^{1/2} = \left(\frac{I_{1.27}^0}{I_{1.27}} \right) = \exp(k_{\text{eff}}[I])t \quad (9)$$

where k_{eff} is a measured rate coefficient equal to $[k_1 k_6 / (k_5 + k_6)] + k_7$ (Section III.C), and t is the time between I_2 injection and $O_2(^1\Sigma)$ monitoring. The I_{6340} cannot be monitored directly since $I_2(B \rightarrow X)$ emission is too great to permit the higher values of I_2 addition, which are of interest. The $I_{1.27}$ can be monitored directly, however. Figure 7 is a plot of the three stages of data reduction: (1) the raw $(I_{7619}/I_{7619}^0 - 1)$ versus $[I]/[O_2(^3\Sigma)]$ data, [Eq. (5)] (Curve A); (2) the data corrected for the gas dynamic reduction of the $[O_2(^1\Delta)]^2$ by use of the results presented in Fig. 6 (Curve B); and (3) doubly corrected data that incorporate the gas dynamic correction and the correction derived from Eqs. (8) and (9) (Curve C). This last plot is roughly linear and yields a value $k_2 = 2.5 \times 10^{10} \text{ cm}^3/\text{mol-sec}$.

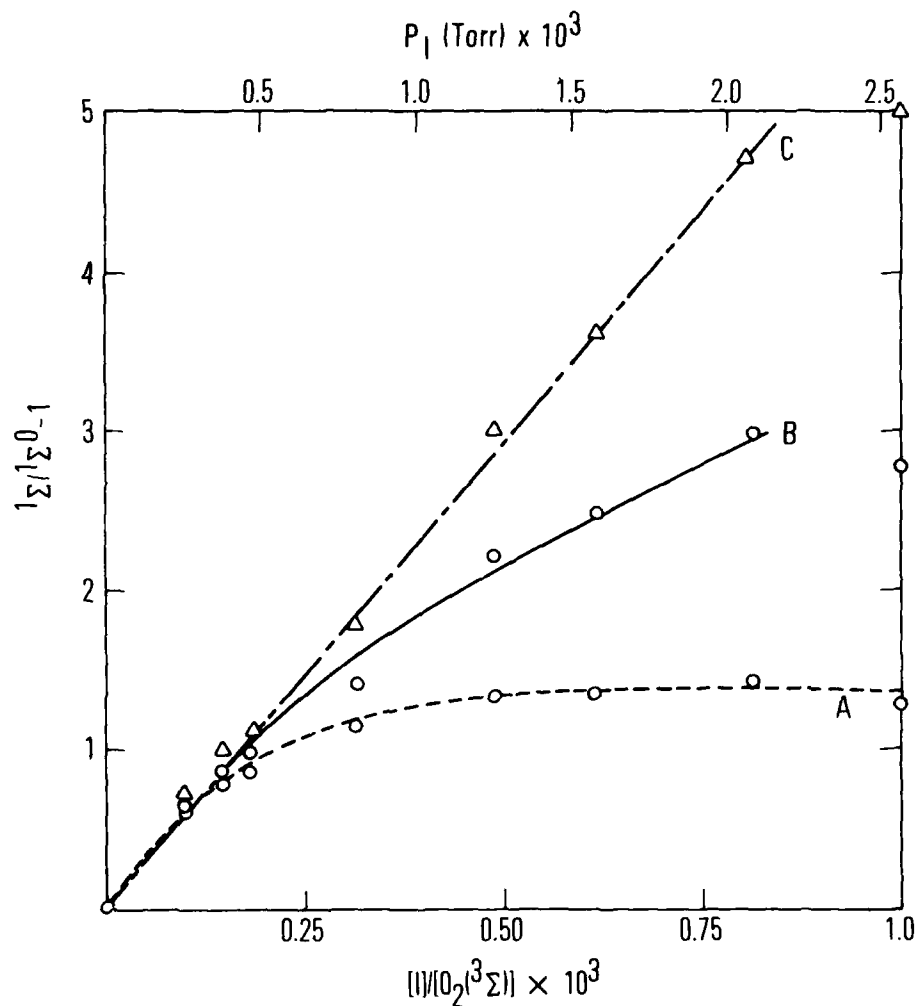
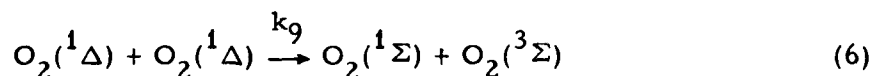


Fig. 7. Determination of k_2 without Saturator Bypass Technique. A, raw data; B, data corrected for gas dynamic effects; C, data corrected for gas dynamic effects and for linear k_{eff} reduction of $O_2(^1\Delta)$.

The second experimental method is much more reliable. As described in the experimental section, the "saturator-bypass" method of controlling the Ar concentration was used. A constant-mass flow rate of Ar was injected into the active O₂, and a varying fraction of this flow was passed through the I₂ saturator. Thus, the total pressure in the system remained constant (to approximately 0.3%), and gas dynamic corrections to partial pressures were eliminated. The fundamental emission signal of O₂(¹Δ) at 1.27 μm is not overlapped by any other spectral feature except for I* at 1.315 μm. This latter problem was eliminated by the use of very narrow slits on the near infrared monochromator. Thus, experimental values of I_{1.27}⁰/I_{1.27} could be provided as input to Eq. (8). At P_{TOT} = 3.67 Torr, k₂ = 5.5 × 10¹⁰ cm³/mol-sec was determined, and at P_{TOT} = 1.69 Torr the result was k₂ = 4.6 × 10¹⁰ cm³/mol-sec (Fig. 8). Therefore, the best value of the I*-O₂(¹Δ) energy pooling rate is

$$k_2 = (5.0 \pm 1.0) \times 10^{10} \text{ cm}^3/\text{mol-sec} \quad (10)$$

where the error reflects the uncertainty in the amount of I₂ added, but not the uncertainty in the quantity k₁/k₉(k₅ + k₆) required to solve Eq. (8). The result is approximately three times faster than that reported by Derwent and Thrush,⁷ i.e., k₂ = (1.6 ± 0.2) × 10¹⁰ cm³/mol-sec. The quantity k₁/(k₅ + k₆) was shown to be closely approximated by the equilibrium constant for Process (1),^{2,7} i.e., K_{EQ} ≡ k₁/k₅ ≃ k₁/(k₅ + k₆). The O₂(¹Δ) energy-pooling rate



has been reliably measured only once,⁴ and any error in that quantity is reflected in the reported value of k₂.

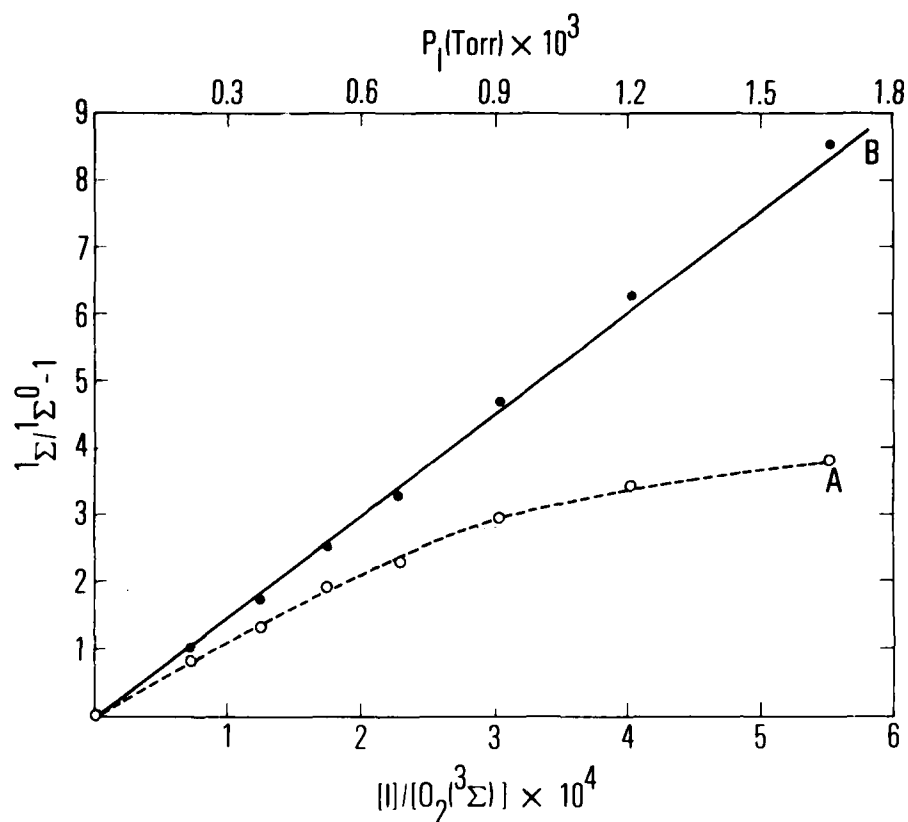


Fig. 8. Determination of k_2 by Use of Saturator Bypass Technique. A, raw data; B, raw data corrected by measured $(I_{1.27}^0/I_{1.27})$, Eq. (8).

The absolute value of k_2 can be viewed in two perspectives from a laser systems point of view. $O_2(^1\Sigma)$ is critical to the operation of the cw $O_2(^1\Delta)$ -I atom transfer laser since it dissociates I_2 with high efficiency. The larger value of k_2 reported here aids this initiation process and removes I_2 as a potential deactivator of I^* . Eventually, k_2 could serve as a pressure-scaling limitation on the transfer laser since this energy-pooling process is second order in $O_2(^1\Delta)$. Note that the " $O_2(^1\Sigma)$ catastrophe" observed in the previous study² is largely eliminated for discharged O_2 by means of the heated saturator and the "saturator-bypass" method. The $^1\Sigma$ catastrophe has been observed in real time in related experiments;* however, for discharged oxygen, it must have an onset at added I_2 pressures greater than 2 mTorr.

C. IODINE-CATALYZED REMOVAL OF $O_2(^1\Delta)$

Derwent and Thrush⁷ reported that the measured removal rate of $O_2(^1\Delta)$ in the presence of I was first order in $[O_2(^1\Delta)]$ and first order in $[I]$. The analytic expression for this kinetic behavior was presented as Eqs. (B-5) and (B-6) in Reference 2.

$$\frac{-d O_2(^1\Delta)}{dt} = \left[\frac{k_1 k_6}{k_5 + k_6} + k_7 \right] [I] [O_2(^1\Delta)] \quad \text{(B-6, Ref. 2)}$$

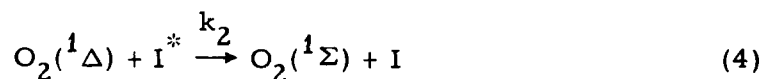
That analysis results in a first-order decay of $O_2(^1\Delta)$ given by

$$\ln \left[\frac{O_2(^1\Delta)^0}{O_2(^1\Delta)} \right] = k_{\text{eff}} [I] t \quad (11)$$

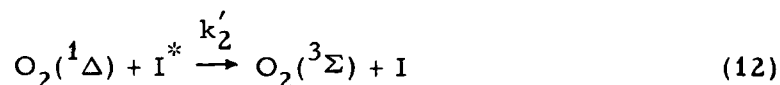
*R. F. Heidner III, unpublished results.

The improved experimental procedures described previously were employed to collect data on the decay of 1.27- μm and 6340- \AA emission in the presence of added I_2 . These data indicate that second-order decay processes in $\text{O}_2(^1\Delta)$ are not negligible at $\text{O}_2(^1\Delta)$ and I-atom densities appropriate for a transfer laser device.

The most interesting second-order loss process for $\text{O}_2(^1\Delta)$ is the energy-pooling reaction with I^* .



The collisions that do not result in $\text{O}_2(^1\Sigma)$ must be considered also, e.g.,



The decay of $\text{O}_2(^1\Delta)$ monitored by the dimol emission at 6340 \AA is shown in Fig. 9. Curvature in the plots is evident although contrary to the prediction of Eq. (11). A second discrepancy with theory is that these plots do not extrapolate well to the intensity at $t = 0$. Unfortunately, dimol emission is a poor diagnostic at high I_2 addition because of interfering $\text{I}_2(\text{B} \rightarrow \text{X})$ emission. Thus, the experiments were continued with $\text{O}_2(^1\Delta)$ fundamental emission at 1.27 μm . In changing of diagnostics, considerable sensitivity to second-order effects is lost because the dimol emission is proportional to $[\text{O}_2(^1\Delta)]^2$, and because the dimol detector (RCA GaAs phototube) is very stable compared to the intrinsic Ge detector used for 1.27- μm radiation. Nevertheless, Fig. 10 is a plot of $\text{I}_{1.27}$ versus time as a function of added I_2 , with it assumed that first-order kinetics apply. Curvature is not evident within experimental error; however, the intercepts are not constant, and, therefore, the linearity may be an artifact of the small dynamic range of

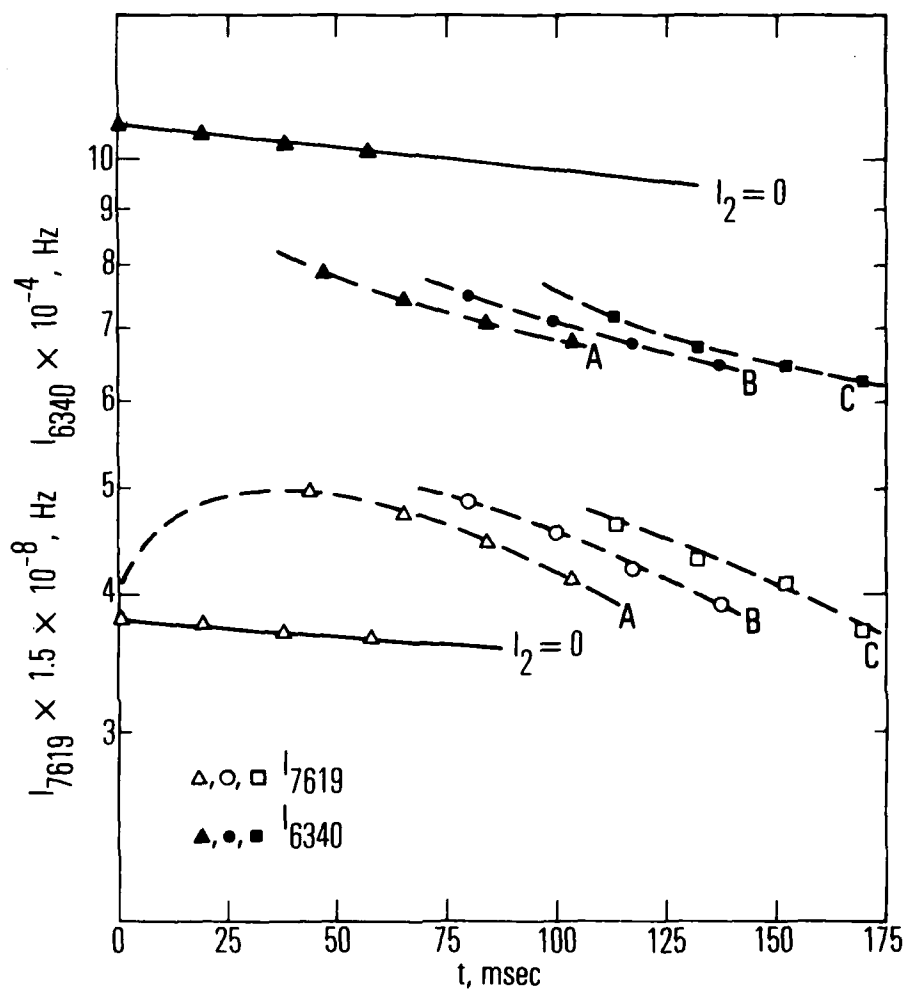


Fig. 9. Time-Dependent $\text{O}_2(^1\Delta)$ Dimol and $\text{O}_2(^1\Sigma)$ Emission in Presence of I_2 . $\text{I} + \text{I}^* = 2.6 \times 10^{-11} \text{ mol/cm}^3$, $\text{O}_2(^3\Sigma) = 1.6 \times 10^{-7} \text{ mol/cm}^3$; $[\text{O}_2(^1\Delta)]_0 = 1.5 \times 10^{-8} \text{ mol/cm}^3$.

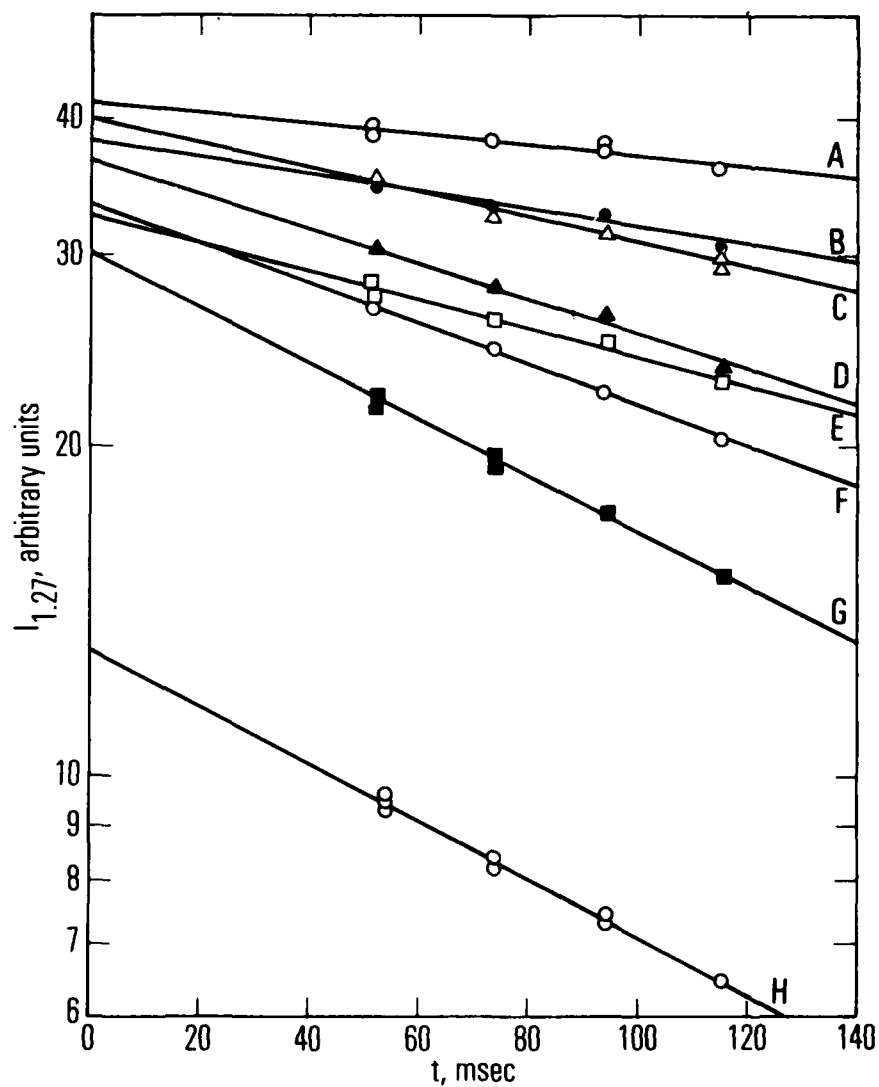


Fig. 10. Time-Dependent First-Order Decay of $O_2(^1\Delta)$ ($\lambda = 1.27 \mu m$) Versus $I_2 \cdot I + I^*$ (mol/cm^3):
A, 0; B, 4.05×10^{-11} ; C, 1.06×10^{-10} ; D, 1.54×10^{-10} ; E, 1.09×10^{-10} ; F, 2.10×10^{-10} ,
G, 3.39×10^{-10} ; H, 4.38×10^{-10} .

$O_2(^1\Delta)$ concentrations measured. If the data are plotted according to Eq. (11), an empirical first-order removal rate of $k_{\text{eff}} = 1.5 \times 10^{10} \text{ cm}^3/\text{mol-sec}$ is derived from Fig. 11. Derwent and Thrush⁷ reported $k_{\text{eff}} = (8.0 \pm 1.0) \times 10^{10} \text{ cm}^3/\text{mol-sec}$.

When the same data are plotted on the basis of second-order kinetics (Fig. 12), the result is extremely interesting. The decay of $O_2(^1\Delta)$ is written as follows:

$$d \frac{O_2(^1\Delta)}{dt} = k[O_2(^1\Delta)][I^*] = 2(k_2 + k'_2)K_{\text{EQ}} \frac{[O_2(^1\Delta)]^2[I]}{[O_2(^3\Sigma)]} \quad (13)$$

$$[O_2(^1\Delta)]^{-1} - [O_2(^1\Delta)]_0^{-1} = 2(k_2 + k'_2)K_{\text{EQ}} \frac{[I]}{[O_2(^3\Sigma)]} t \quad (14)$$

The intercept variation in Fig. 12 may be within experimental error, and the linearity is no worse than that in Fig. 10, in which first-order kinetics is assumed. With the measured value of $[O_2(^1\Delta)]_0^{-1}$ inserted into Eq. (14), the quantity $2(k_2 + k'_2) \approx 1.3 \times 10^{11} \text{ cm}^3/\text{mol-sec}$ is determined (Fig. 13). Given the assumptions involved, this value is rather close to the value of $k_2 = (5.0 \pm 1.0) \times 10^{10} \text{ cm}^3/\text{mol-sec}$, which was determined by a completely different method. Data over a much larger dynamic range would be required in order to accurately deconvolute the first- and second-order components of the decay of $O_2(^1\Delta)$. The results of these studies are compared with earlier results in Table III.

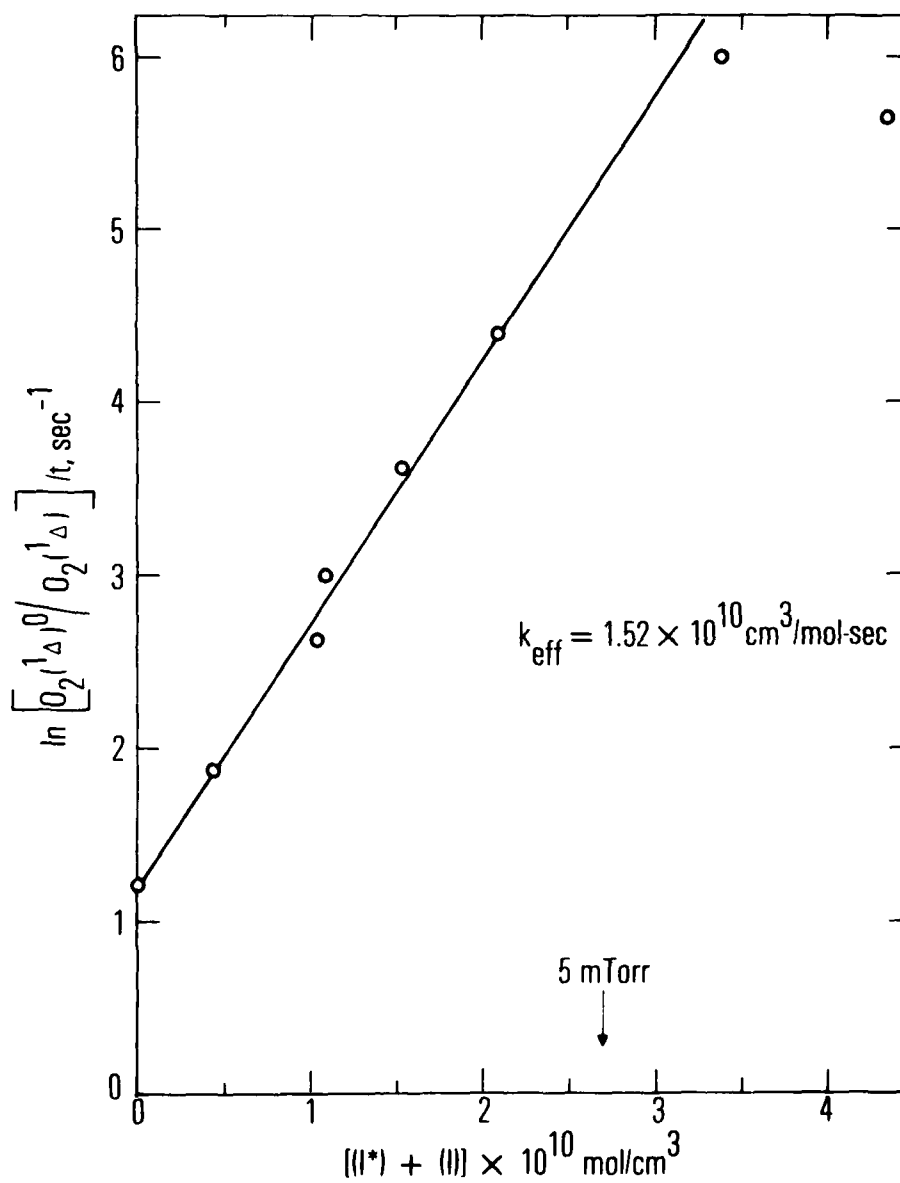


Fig. 11. Determination of k_{eff} with First-Order Decay of $O_2(^1\Delta)$ Assumed

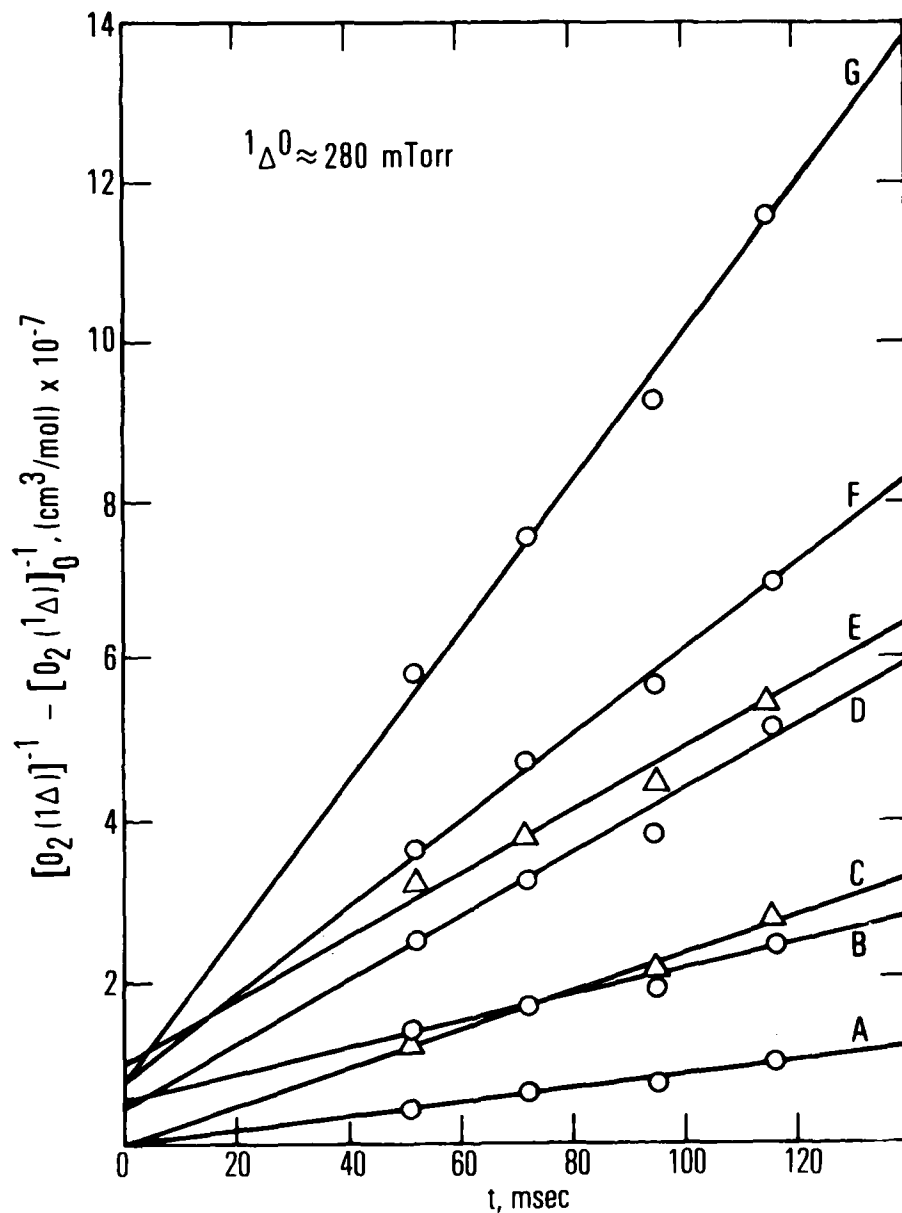


Fig. 12. Time-Dependent Second-Order Decay of $\text{O}_2(^1\Delta)$ ($\lambda = 1.27 \mu\text{m}$) Versus $\text{I}_2 \cdot \text{I} + \text{I}^*$ (mol/cm^3): A, 0; B, 4.05×10^{-11} ; C, 1.06×10^{-10} ; D, 1.09×10^{-10} ; E, 1.54×10^{-10} ; F, 2.10×10^{-10} ; G, 3.39×10^{-10} ; H, 4.38×10^{-10} .

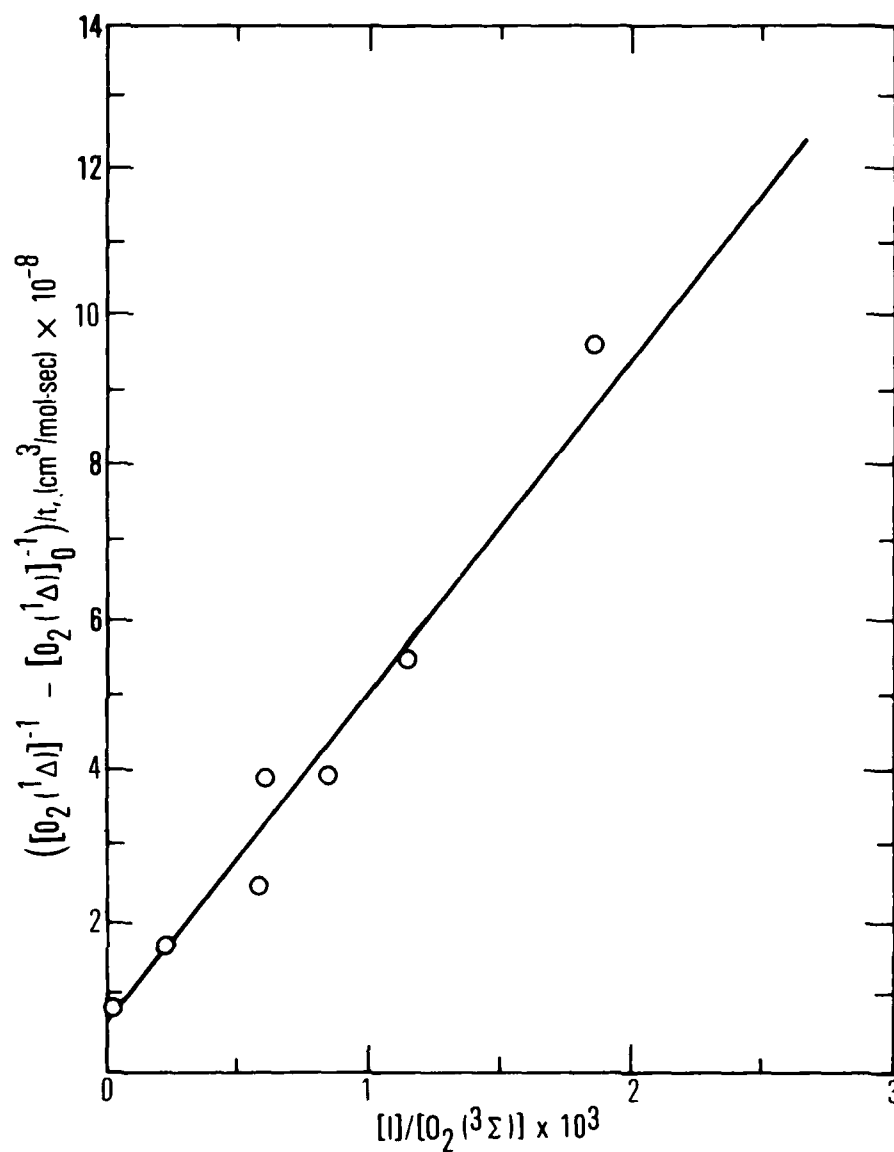


Fig. 13. Determination of $k_2 + k'_2$ with Second-Order Decay Kinetics Assumed for $O_2(^1\Delta)$

Table III. Comparison of Kinetic Results

Process, cm ³ /mol-sec	Derwent and Thrush	Reference 2	This Work
k_2^a	$(1.6 \pm 0.2) \times 10^{10}$	1.3×10^{10}	$(5.0 \pm 1.0) \times 10^{10}$
$k_{\text{eff}} \left\{ \equiv k_6 \left[\frac{k_1}{(k_5 + k_6)} \right] + k_7 \right\}$	$(8 \pm 1) \times 10^{10}$	--	$1.5 \times 10^{10}{}^b$
$k \left \equiv 2(k_2 + k_2') \right\}$	--	--	$1.3 \times 10^{11}{}^c$

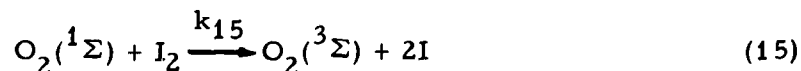
^aDetermined from $(k_2/k_9) [k_1/(k_5 + k_6)]$.

^bWith first-order kinetic loss of $O_2(^1\Delta)$ assumed.

^cWith second-order iodine-catalyzed removal of $O_2(^1\Delta)$ assumed.

IV. DISCUSSION

The efficient operation of the cw $O_2(^1\Delta)$ -I atom transfer laser requires a kinetic environment consisting of high concentrations of $O_2(^1\Delta)$ and I^* . Since I^*/I must be greater than 0.5 in order to exhibit laser action, kinetic studies must distinguish the effects of ground-state and excited-state I atoms. I^* to I ratios higher than those used by Derwent and Thrush⁷ were used in these studies, which may explain the differences in Table III. Measurements of the energy-pooling rate k_2 between $O_2(^1\Delta)$ and I^* tend to be low unless the accelerated decay of $O_2(^1\Delta)$ by iodine is explicitly accounted for by Eq. (8). Thus, the present value of $(5.0 \pm 1.0) \times 10^{10}$ cm³/mol-sec is strongly favored over earlier measurements.^{2,7} Even this value could be systematically in error if k_9 were incorrectly determined. The large value for k_2 is supported by the rapid dissociation of injected I_2 by $O_2(^1\Sigma)$



The iodine-catalyzed removal of $O_2(^1\Delta)$ is a much more complicated question. The results of the present study support a substantial contribution to the decay of $O_2(^1\Delta)$, which is proportional to $[O_2(^1\Delta)]^2$. The following is a numerical example of the difference between first- and second-order kinetics. The experimental conditions are typical of the recent laser¹ experiments; in addition, the I^* and $O_2(^1\Delta)$ densities are comparable to the present studies.

$$[O_2(^1\Delta)]_0 = 1.5 \times 10^{-8} \text{ mol/cm}^3 \text{ (280 mTorr)}$$

$$[I] + [I^*] = 3.0 \times 10^{-10} \text{ mol/cm}^3 \text{ (6 mTorr)}$$

$$\frac{[\text{O}_2(^1\Delta)]}{[\text{O}_2(^3\Sigma)]} = 0.4$$

$$\frac{[\text{I}^*]}{[\text{I}]} = 1.2$$

The first-order half-life of $\text{O}_2(^1\Delta)$ can be expressed as

$$\begin{aligned}\tau_{1/2} &= (\ln 2)(k_{\text{eff}}[\text{I}])^{-1} \\ &= 62 \text{ msec (Derwent and Thrush)} \\ &= 340 \text{ msec (this work)}\end{aligned}\tag{16}$$

The second-order half-life of $\text{O}_2(^1\Delta)$ can be expressed as

$$\begin{aligned}\tau_{1/2} &= \left[2(k_2 + k'_2)[\text{I}^*]_0 \right]^{-1} \\ &= 28.3 \text{ msec (this work)}\end{aligned}\tag{17}$$

The predicted second-order half-life for $\text{O}_2(^1\Delta)$ would appear to be the correct order of magnitude to describe the laser operation. Even the large k_{eff} for first-order decay given by Derwent and Thrush⁷ results in a relatively slow decay. Three scaling cases must be considered:

1. The $[\text{O}_2(^1\Delta)]/[\text{O}_2(^3\Sigma)]_0$ could be increased, which would improve the mass efficiency of the laser but would also increase the decay rate by increasing $[\text{I}^*]$ prior to the optical cavity. Fast, efficient mixing would be imperative.
2. The $[\text{O}_2(^1\Delta)]/[\text{O}_2(^3\Sigma)]_0$ ratio could remain constant, but the total O_2 pressure could be increased. The decay rate would remain constant if the $[\text{I}] + [\text{I}^*]$ remained constant.
3. The $[\text{I}] + [\text{I}^*]$ could be increased to enhance the gain and improve the energy extraction. This technique could accelerate the $\text{O}_2(^1\Delta)$ loss rate to unacceptable levels.

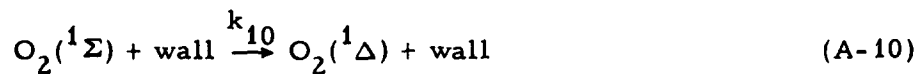
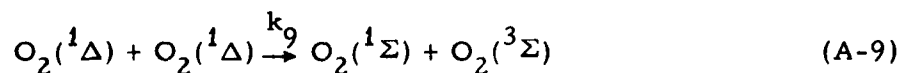
Gain length scaling may be required rather than $[I^*]$ scaling in order to increase overall system gain. Scaling from $[O_2(^1\Delta)]/[O_2(^3\Sigma)] = 0.4$ to $[O_2(^1\Delta)]/[O_2(^3\Sigma)] = \infty$ increases the decay rate of $O_2(^1\Delta)$ less than a factor of 2 and should be pursued if technically feasible. Increasing the pressure of the $O_2(^1\Delta)$ is very desirable unless the Derwent and Thrush⁴ value for k_9 is much lower than the actual value. Experiments on the decay rate of $O_2(^1\Delta)$ in pure oxygen system strongly support the Derwent and Thrush value.

V. CONCLUSIONS

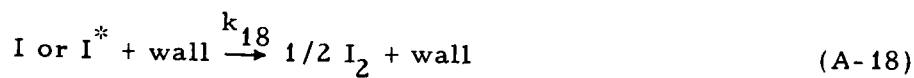
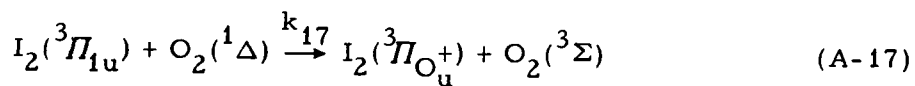
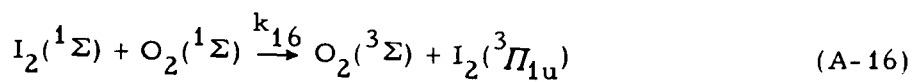
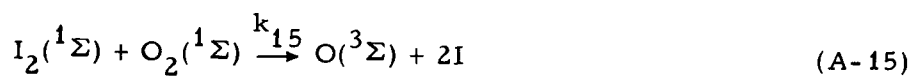
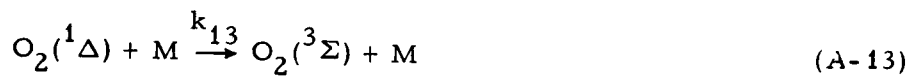
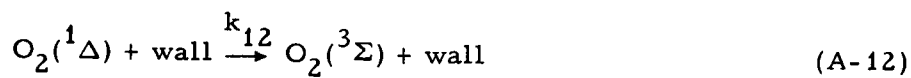
Modification of the Derwent and Thrush³⁻⁷ kinetic rate package is necessary because the $O_2(^1\Delta)$ - I^* energy-pooling rate is substantially faster than these authors have proposed. Furthermore, collisions between $O_2(^1\Delta)$ and I^* , resulting in kinetics that are second order in $O_2(^1\Delta)$, may dominate the removal of $O_2(^1\Delta)$ at densities appropriate to the transfer laser. This area of the kinetics, which includes temperature-dependent measurements, is of critical importance in accurate laser modeling.

APPENDIX A

CHEMICAL KINETICS OF THE $O_2(^1\Delta)$ -I ATOM SYSTEM^a



^aWhere possible, the above reactions are numbered as they appear in Reference 7.



APPENDIX B

RATE COEFFICIENTS FOR THE KINETIC MODEL OF APPENDIX A

Process	k	Reference
k_1	$(4.6 \pm 1.5) \times 10^{13} \text{ cm}^3/\text{mol-sec}$	2
k_2	$(1.6 \pm 0.2) \times 10^{10} \text{ cm}^3/\text{mol-sec}$	7
	$(5 \pm 1) \times 10^{10} \text{ cm}^3/\text{mol-sec}$	This Work
$k_2 + k'_2$	$6.5 \times 10^{10} \text{ cm}^3/\text{mol-sec}$	This Work
k_3	7.8 sec^{-1}	2
k_4	0.077 sec^{-1}	2
k_5	$(1.6 \pm 0.5) \times 10^{13} \text{ cm}^3/\text{mol-sec}$	2
k_6	$3.4 \times 10^{10} \text{ cm}^3/\text{mol-sec}$	2
k_7	$8 \times 10^{10} \text{ cm}^3/\text{mol-sec}$	2
k_8		
k_9	$1.2 \times 10^7 \text{ cm}^3/\text{mol-sec}$	2
k_{10}	$\gamma_{10} \approx 1 \times 10^{-2}$	2
k_{11}	$\gamma_{11} \approx 1$	2
k_{12}	$\gamma_{12} \approx 2 \times 10^{-5}$	2
k_{13}		
k_{14}		
k_{15}	$1 \times 10^{14} \text{ cm}^3/\text{mol-sec}$	2
k_{16}	$4 \times 10^{13} \text{ cm}^3/\text{mol-sec}$	2
k_{17}		
k_{18}	$\gamma_{18}(\text{Pyrex}) \approx 1; \gamma_{18}(\text{Halocarbon}) \approx 10^{-3}$	2